Progress In Electromagnetics Research C, Vol. 116, 1–12, 2021

Design and Realization of Dual Band Notch UWB MIMO Antenna in 5G and Wi-Fi 6E by Using Hybrid Technique

Hamza El Omari El Bakali[1, *], Alia Zakriti[2], Abdelkrim Farkhsi[1], Aziz Dkiouak[2], and Mohssine El Ouahabi[2]

Abstract—In this paper, a novel design of a small printed Ultra-Wideband (UWB) Multi-Input Multi-Output (MIMO) antenna with a wide impedance bandwidth from 3.05 GHz to 11.65 GHz is introduced. The newly designed UWB MIMO antenna has an isolation enhancement of more than −15 dB between the two elements. This isolation is achieved by inserting a three-line stub on the ground plane between the two radiating elements. In addition, these parallel lines improve the impedance matching and the bandwidth of this structure. Dual band notched characteristics are achieved for the 5G band (3.6 GHz) and Wi-fi 6E application (6 GHz), by etching a complementary split ring resonator (CSRR) in both the truncated square patch elements and by loading the split ring resonator (SRR) on the ground plane at the back of antenna, respectively. The SRR and its complement are metamaterials structures, showing the behavior of an LC resonator circuit. The hybrid technique improves impedance matching, bandwidth, minimizes the mutual coupling in UWB frequency range, and delivers dual-notch characteristics. The simulation and measurement results of the proposed antenna with a good agreement are presented. The proposed structure exhibits high performances in terms of envelope correlation coefficient (ECC), diversity gain (DG), efficiency, total active reflection coefficient (TARC), and channel capacity loss (CCL) except the notched band.

1. INTRODUCTION

Today's modern wireless communications sector is very demanding and requires both high data transmission speed and good quality of service. For a wide range of applications, including short-range radar, imaging systems, and broadband wireless applications, UWB is a very attractive technology due to its low cost, low power level, and high data rate [1, 2]. However, besides all these positive characteristics, UWB system is also affected by transmission problems such as multipath fading. The integration of MIMO technique in UWB systems is seen as the key to increasing channel capacity and reducing multipath fading without the need for additional power [3–6].

Increasing attention has been paid to the design of a compact UWB MIMO antenna suitable for portable wireless devices. However, the placement of multiple antenna elements on the receiving terminal in a limited space causes considerable problems such as mutual coupling between the adjacent antenna elements [7]. Therefore, several recent techniques and procedures have been suggested in the literature to overcome this limitation by maintaining the overall size of the MIMO such as the use of parasitic elements between the antennas on both sides of the substrate which yields an insertion loss lower than −20 dB in the operational frequency band [8], In Ref. [9], an arc-shaped Defected Ground Structure (DGS) is embedded in the ground plane to reduce the mutual coupling effect between the

Received 7 August 2021, Accepted 15 September 2021, Scheduled 9 October 2021

* Corresponding author: Hamza El Omari El Bakali (h.elomari@uae.ac.ma).

[1] Department of Physics, Information Systems and Telecommunications Laboratory, Faculty of Science, Abdelmalek Essaadi University, Tetuan, Morocco. [2] Department of Civil and Industrial Sciences and Technologies, Laboratory of Sciences and Advanced Technology, National School of Applied Sciences, Abdelmalek Essaadi University, Tetuan, Morocco.

feed lines, and the mutual coupling value can be suppressed up to a level of −37.5 dB in the band of operation. Another approach to the insertion of the neutralization line is presented in [10], and this technique improves the isolation between two symmetrical antennas by more than 25 dB. In addition, a compact Uniplanar Electromagnetic Band Gap (UC-EBG) UWB MIMO antenna is reported in [11], where the isolation is better than −18 dB over the complete impedance bandwidth.

However, the existence of several narrowband wireless networks, such as 5G with a center frequency of 3.6 GHz or Wi-Fi 6E with a center frequency of 6 GHz, may cause significant interference in the FCC-allocated UWB radio spectrum (3.1–10.6 GHz). This problem can be solved by introducing band stop filter circuits into UWB devices, but this increases the system cost and size [12]. Numerous UWB-MIMO antenna designs with band notch behavior have been reported [13–16]. In [13], a U-shaped slot is inserted on the surface of the antenna element to obstruct the current distribution at 5.5 GHz. In [14], the authors achieve dual band rejection-characteristics of Wi-MAX (3.5 GHz) and WLAN (5.5 GHz) by loading two independent slits on each antenna element. In [15], a triple band rejection phenomenon is achieved by etching rotated C-shaped slots on the patches and rectangular slots on the ground planes. Another approach using metamaterial structures (ELC) was the main idea for the design of a UWB antenna in [16] for making notches resonance. Depending on their topology, SRRs and their complements exhibit the behavior of an LC resonator circuit and are modelled using Nicolson-Ross or transmission/reflection techniques to extract permittivity and permeability [17]. The challenge is to design a planar antenna with a compact size, multi-band rejection capability, and low mutuality.

In this paper, a CPW-fed 2×2 UWB MIMO antenna with a total area of (40 mm×30 mm) is proposed to provide dual band notch characteristics in the operational frequency band from 3.05 GHz to 11.65 GHz. The design process starts with designing a UWB MIMO antenna based on the classical square patch. In the second step, a three-line stub is incorporated between the antenna elements to improve impedance matching and reduce mutual coupling. Finally, to create dual-band notch rejection at the 5G band (3.6 GHz) and the Wi-fi 6E application (6 GHz), a complementary split ring resonator (CSRR) is etched on the truncated square planar monopoles while the split ring resonator (SRR) is loaded on the ground plane at the back of each patch antenna, respectively. This paper proposes a new design of a UWB MIMO antenna which is characterized by a simple structure and small size. The configuration of the suggested antenna system is presented in detail in the following section.

All electromagnetic simulations and designs were carried out using CST Microwave Studio®(CST MWS) software, which is a specialized tool for 3D electromagnetic simulation of high frequency components. CST MWS is based on the Finite Integration Technique (FIT) and allows a fast and accurate analysis of high frequency (HF) devices such as antennas.

The benefits and novelties of the proposed dual notch band UWB MIMO antenna are briefly listed as follows:

(i) **Simplicity:** The structure is very simple. It is conceived and fabricated on a thin Rogers substrate with less losses. It minimizes the complexity of the system; then it can be easily installed in different communication systems applications.

(ii) **Miniaturization:** The proposed structure delivers UWB performance with double notched bands characteristics in a compact size of ($40\times30\times0.64\,\text{mm}^3$) using the hybrid technique.

(iii) **Good reflection coefficient:** The reflection coefficient of the proposed antenna is less than −1 dB in the whole, except for the notched band characteristic. The value of this coefficient ensures a better impedance matching, and thus the radiation power is enough.

(iv) **Low mutual coupling**: A high isolation of more than −15 dB within the whole wide bandwidth is achieved between the two elements. This isolation is obtained within a restricted space for a two-port MIMO antenna array by using multi-parallel lines isolating element and spit ring resonator.

(v) **Ultra-wideband**: Ultra-wideband communication systems provide a very high bandwidth, which covers the bandwidth requirement of multiples applications (Imaging applications and X band RADAR...). In addition, UWB reduced fading from multipath and low power requirements.

(vi) **Two band notch characteristics:** The introduction of both CSRR & SRR resonators produces dual-band notch characteristics. The presence of two stopbands eliminates the interference with 5G (recognized internationally as a pioneer band for 5G services) from 3.30 GHz to 3.80 GHz and the Wi-Fi 6E (That stands for Wi-Fi 6 extended into the 6 GHz band) from 5.945 GHz to 6.425 GHz.

(vii) **Novelty:** In this paper, a combination of a novel technique multi-parallel lines isolating element, SRR, and CSRR was being carried out to enhance the isolation, impedance matching, bandwidth, and to create two new frequency bands rejected mechanism, which are used to alleviate the electromagnetic interference with two vital applications involving the next generation 5G and Wi-Fi 6E.

2. TWO-ELEMENT MIMO ANTENNAS DESIGN

The geometry of the proposed UWB MIMO antenna with two frequency rejection characteristics is shown in Figure 1. The design process starts with the design of a CPW-fed MIMO UWB antenna with two symmetrical truncated square patches and a modified partial ground plane to provide wide frequency response. A three-line stub is incorporated into the upper ground plane in order to improve the impedance matching, bandwidth, and isolation between the two antenna elements over the entire bandwidth. In order to create dual-band notch rejection at the 5G band (3.6 GHz) and the Wi-fi 6E application (6 GHz), a CSRR is etched on the patch elements while an SRR is loaded on the ground plane at the back of each radiating element, respectively. The proposed structure was printed on a Rogers RT6010 substrate with a thickness of 0.64 mm, a dielectric constant ε_r of 10.2, and a tangent loss (tan δ) of 0.0023. The designed UWB MIMO antenna features a compact size of $40\times30\,\text{mm}^2$, and the all-physical dimensions are given by Table 1.

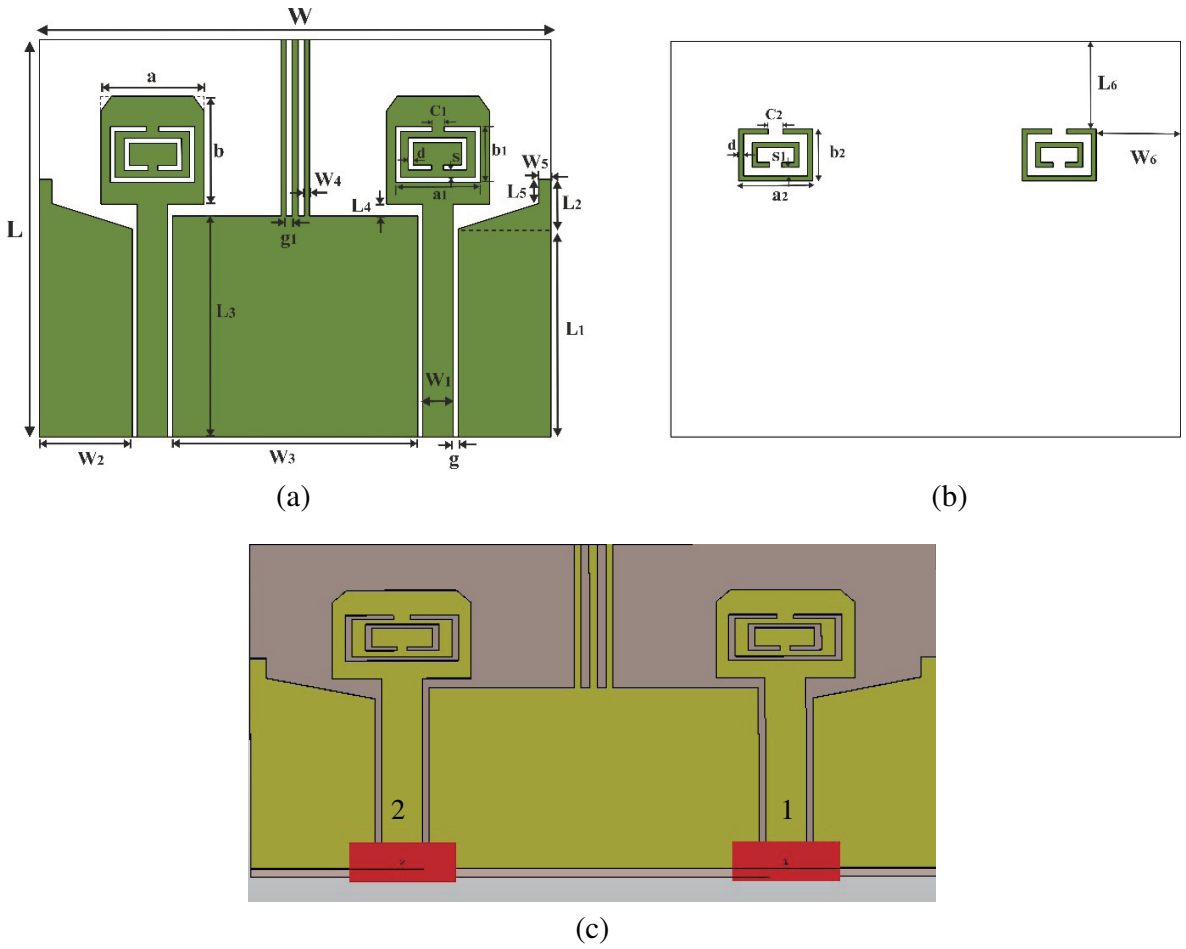

Figure 1. Proposed MIMO antenna: (a) Geometry of top view, (b) geometry of bottom view (c) structure with waveport in CST.

Table 1. The entire dimensions of the proposed UWB MIMO antenna.

Parameters	W	L	W_1	W_2	W_3	W_4	W_5	W_6	L_1	L_2	L_3	L_4	L_5	L_6
Values (mm)	40	30	2.45	7.5	18.5	0.4	1	6	16.8	4	17.8	1	2	7
Parameters	g	g_1	a	a_1	a_2	b	b_1	b_2	C_1	C_2	d	S	S_1	h
Values (mm)	0.4	0.5	8.5	6.8	6	8.5	4.5	4.2	1	1.2	0.4	0.6	0.7	0.64

3. EVOLUTION DESIGN OF DOUBLE BAND NOTCH UWB MIMO ANTENNA

The design evolution steps of the proposed dual-band notched MIMO UWB antenna element are shown in Figure 2. The design process starts with the conception of a wide band MIMO antenna based on the classical truncated square patch and a modified partial ground plane (Figure 2 (Ant.0)). The -10 dB impedance bandwidth of this configuration varies from 3.5 to 11.2 GHz with low isolation on the whole bandwidth. For the impedance matching, bandwidth, and isolation improvement, three-line stubs have been loaded in the center of the upper part of the ground plane. The multi-parallel lines act as a resonator to generate transmission zeros between the two antennas. The corresponding results are shown in Figure 2 (Ant.1) and indicate that the -10 dB bandwidth reaches 3.16–11.4 GHz. Moreover, to reduce signal interference, two band notches are achieved at 3.6 and 6 GHz in the UWB range by inserting the CSRR on the radiator patch, while the SRR is loaded on ground plane at the back of the antenna respectively (Figure 2 (Ant.2)).

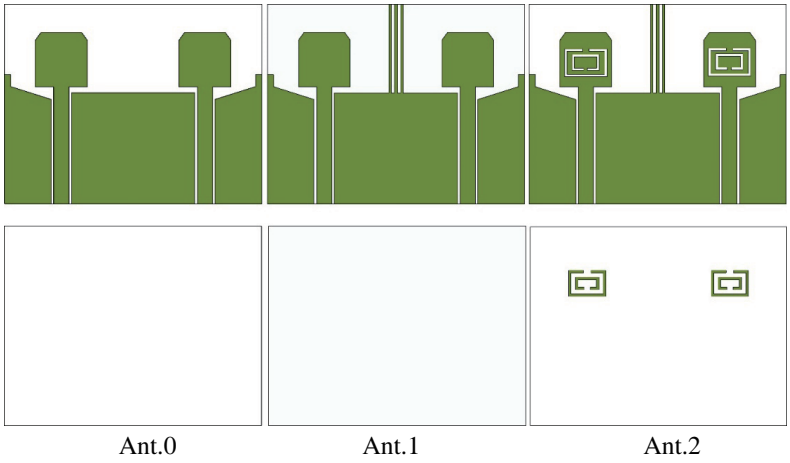

Figure 2. Evolution design of the proposed UWB MIMO antenna.

It is clearly seen from Figure 3 (Ant.2) that the two resonators SRR and CSRR slightly affects the impedance matching beyond the frequency of 7.5 GHz but does not affect the performance of the impedance bandwidth or the isolation other than two notched bands. In addition to that, both the resonators improve the isolation more than -2 dB in the whole operating band.

4. RESULTS AND DISCUSSION

4.1. Current Distribution

In this section, the study of the current distribution has been added to highlight the importance of using the metamaterials resonators for filtering selected frequency bands. On the one hand, the current is mainly focused on the CSRR in the top layer and is very low in the rest of the structure for the first rejected band at 3.6 GHz, as shown in Figure 4(a). On the other hand, the current is mainly

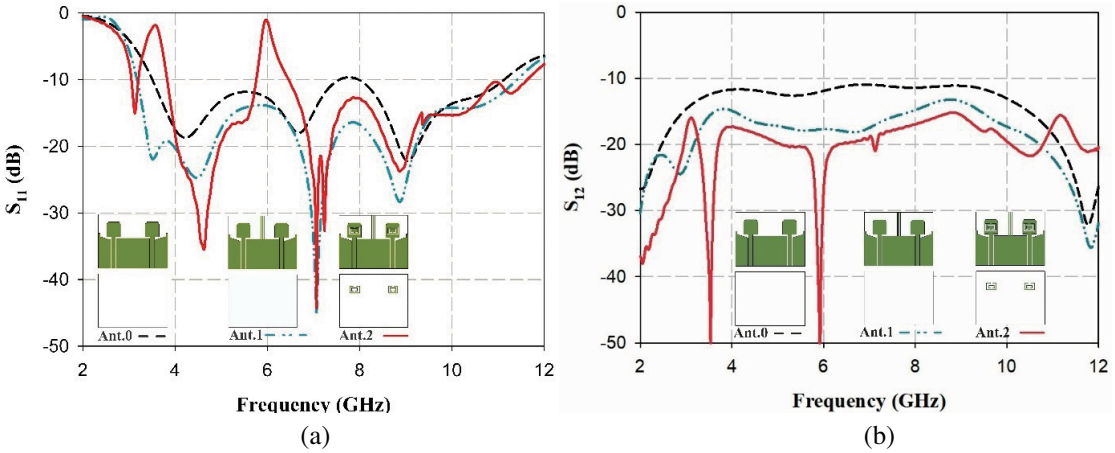

Figure 3. S-parameters of three different antennas: (a) S_{11}, (b) S_{21}.

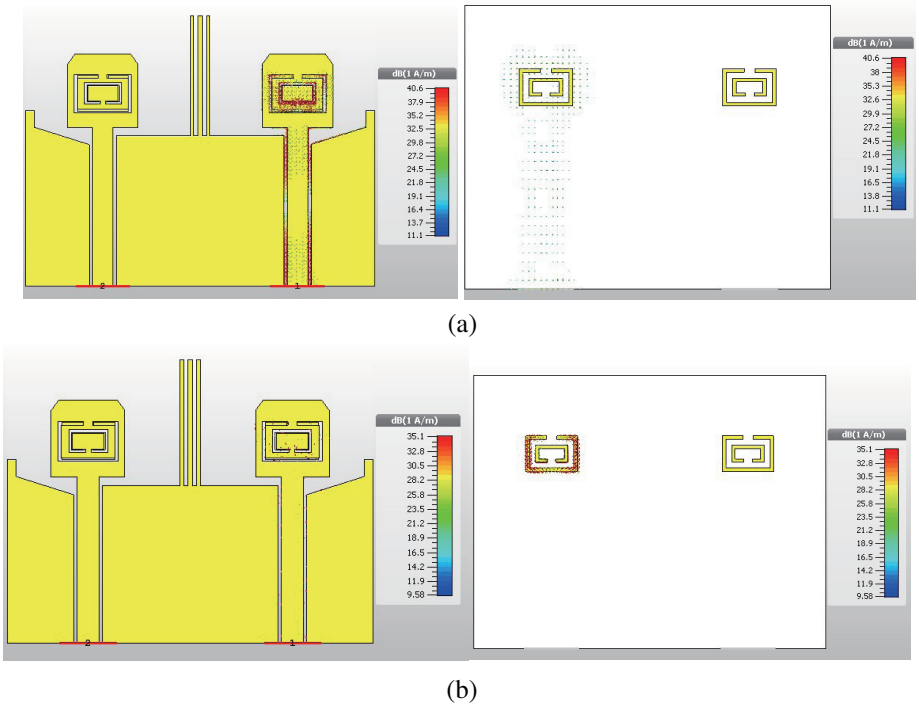

Figure 4. Simulated surface current distribution while feeding only Port 1 at (a) 3.6 GHz (b) 6 GHz.

concentrated over the SRR in the bottom layer for the second rejected band at 6 GHz, as shown in Figure 4(b). From this current distribution study, we notice the importance of the use of the resonators (CSRR and SRR) in the rejection of the two undesirable bands.

4.2. Experimental Results

The presented dual band notched UWB MIMO antenna is fabricated, tested, and measured by using Rohde and Schwarz ZVB 20 vector network analyzer. The fabricated prototype of this structure with top and bottom views and its S-parameters are illustrated in Figures 5 and 6, respectively.

From Figure 6, the measured reflection coefficient has a wide impedance bandwidth from 3.45 to 10.83 GHz with dual band notched characteristics. The center frequency of the two notch bands reject interference due to the future fifth generation (5G) mobile networks, and the Wi-Fi 6E bands

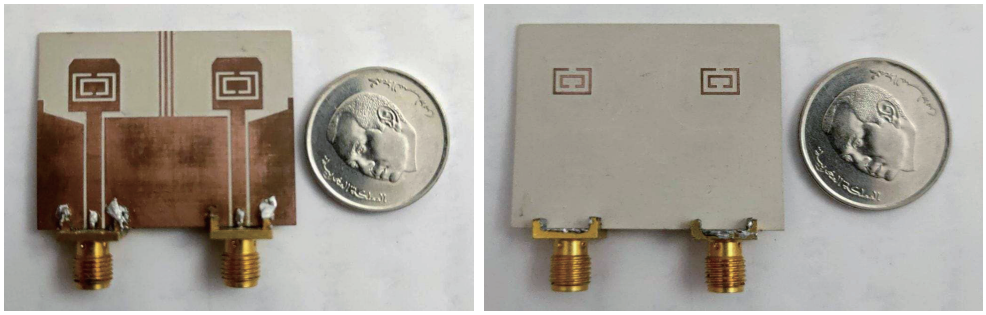

(a) (b)

Figure 5. Proposed double notch band UWB-MIMO antenna fabricated prototype (a) top view, (b) bottom view.

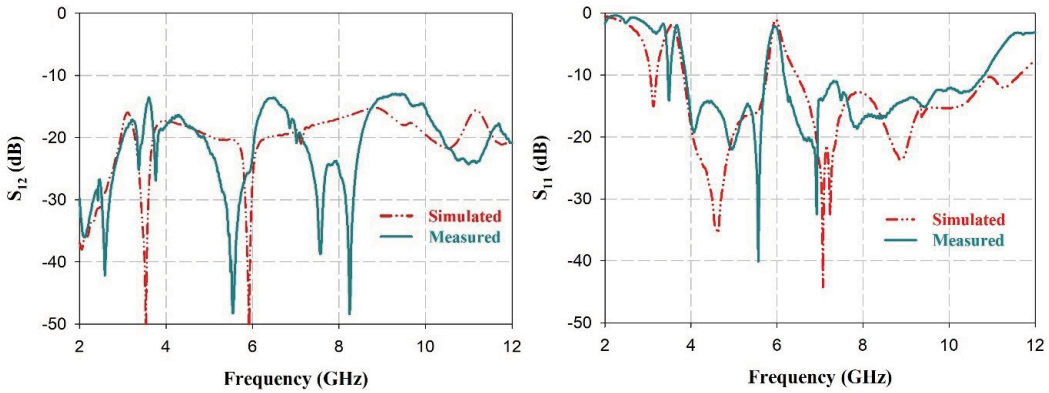

(a) (b)

Figure 6. Measured and simulated S-parameters of the proposed double notch band UWB-MIMO antenna.

are 3.65 GHz (3.4–3.9 GHz) and 5.92 GHz (5.7–6.2 GHz), respectively. The measured mutual coupling is more than −13.5 dB at the entire frequency range. The measured and simulated results are in good agreement. There is a little shift in the frequency range of the notched band due to minor fabrication tolerances or unavoidable conductor loss in the usage of coaxial cables at the time of measurements. Comparison of simulated and measured results is tabulated in Table 2 given below.

Table 2. Comparison of the simulated and measured results.

	Operating Bandwidth (GHz)	Notched Bandwidth (GHz)		Isolation(dB)
		Lower notch	Higher notch	
Simulated	3.05–11.65	3.5	6	−15
Measured	3.45- 10.83	3.65	5.92	−13.5

5. MIMO PERFORMANCE PARAMETERS

The performance of the proposed dual notched band MIMO antenna configuration in terms of ECC, DG, efficiency, TARC, and CCL is discussed in detail in the following subsection.

5.1. Envelope Correlation Coefficient and Diversity Gain

The ECC between the adjacent radiating elements ith and jth for N-port MIMO antenna system using far-field patterns [16] is given by Equation (1):

$$ECC\left(i,j\right)=\frac{\left(\oint\left(X_{PR}E_{\theta i}\left(\Omega\right)E_{\theta j}^{*}\left(\Omega\right)P_{\theta}\left(\Omega\right)+E_{\phi i}\left(\Omega\right)E_{\phi j}^{*}\left(\Omega\right)P_{\phi}\left(\Omega\right)\right)d\left(\Omega\right)\right)^{2}}{\oint\left(X_{PR}G_{\theta i}(\Omega)P_{\theta}(\Omega)+G_{\phi i}(\Omega)P_{\phi}(\Omega)\right)d(\Omega)\cdot\oint\left(X_{PR}G_{\theta j}\left(\Omega\right)P_{\theta}\left(\Omega\right)+G_{\phi j}\left(\Omega\right)P_{\phi}\left(\Omega\right)\right)d\left(\Omega\right)} \tag{1}$$

where X_{PR} denotes the cross-polarization power ratio of the propagation environment. In the above formula, $G_{\theta}\left(\Omega\right)=E_{\theta}\left(\Omega\right)E_{\theta}^{*}\left(\Omega\right)$ and $G_{\phi}\left(\Omega\right)=E_{\phi}\left(\Omega\right)E_{\phi}^{*}\left(\Omega\right)$ are the power patterns of θ and ϕ polarizations, respectively. $P_{\theta}\left(\Omega\right)$ and $P_{\phi}\left(\Omega\right)$ denote the angular density functions of the θ and ϕ polarizations, respectively. $E_{\theta i}\left(\Omega\right)$ and $E_{\theta j}\left(\Omega\right)$ are the electric field patterns of the ith and jth antenna elements in the θ polarization, respectively. $E_{\phi i}\left(\Omega\right)$ and $E_{\phi j}\left(\Omega\right)$ are the electric field patterns of the ith and jth antenna elements in the ϕ polarization, respectively.

For uniform multipath environment, $X_{PR}=1$ and $P_{\theta}\left(\Omega\right)=P_{\phi}\left(\Omega\right)=\frac{1}{4\pi}$.

The ECC for two antennas can be approximated as follows [18]:

$$ECC=\frac{\left(\oint\left(E_{\theta1}\left(\Omega\right)E_{\theta2}^{*}\left(\Omega\right)+E_{\phi1}\left(\Omega\right)E_{\phi2}^{*}\left(\Omega\right)\right)d\left(\Omega\right)\right)^{2}}{\oint\left(G_{\theta1}\left(\Omega\right)+G_{\phi1}\left(\Omega\right)\right)d\left(\Omega\right)\cdot\oint\left(G_{\theta2}\left(\Omega\right)+G_{\phi2}\left(\Omega\right)\right)d\left(\Omega\right)} \tag{2}$$

where E_1 and E_2 are the far-field radiation patterns, generated from ports 1 and 2, respectively. The DG of proposed MIMO antenna [19, 20] is given by the following expression:

$$\mathrm{DG}=10\sqrt{1-\left|\rho\right|^{2}} \tag{3}$$

where ρ is the complex cross correlation coefficient, and $\left|\rho\right|^{2}\approx ECC$.

The simulated and measured ECC and DG graphs are illustrated in Figure 7. The simulated results in terms of ECC and DG are obtained from the radiation patterns, while the measured results are obtained from the S-parameters.

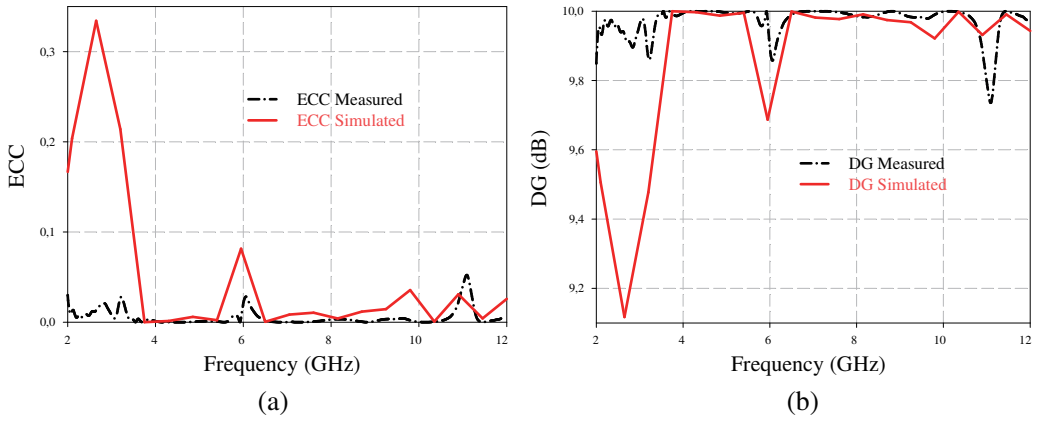

Figure 7. Diversity Performance: (a) ECC and (b) DG.

As can be seen from Figure 7(a), the ECC is less than 0.03 for the entire UWB radiating bands, except at the two notched bands (3 to 4.4 GHz and 5.5 to 6.5 GHz), where the ECC increases to 0.35, while the DG is greater than 9.75 dB except the notched band as depicted in Figure 7(b).

5.2. Efficiency

The simulated radiation efficiency is about 15% in the first notch band and about 15% in the second notch band as depicted in Figure 8. A high radiation efficiency above 67% advocates almost stable performance of the proposed dual band notch UWB-MIMO antenna.

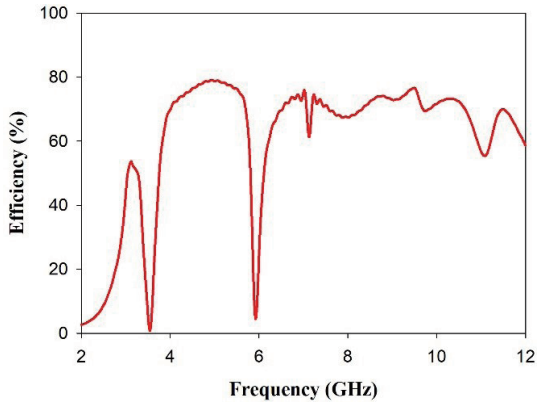

Figure 8. Efficiency of the proposed design.

5.3. Total Active Reflection Coefficient

For a two-port MIMO system, $i = 1$, $j = 2$, and $N = 2$, the TARC is calculated using the S-parameters [19] by the following equation:

$$TARC = \sqrt{\frac{|(S_{11} + S_{12}e^{j\theta})|^2 + |(S_{22} + S_{21}e^{j\theta})|^2}{2}} \tag{4}$$

where θ is the Gaussian random input feed phase, and it ranges from 0 to π.

This parameter is less than -10 dB in the entire frequency range except the notch characteristics in 5G and WiFi 6E bands as can be seen in Figure 9. The small difference between the simulated and measured results is especially due to the effect of soldering the SMA connectors and the tolerance levels during the fabrication process of the antenna.

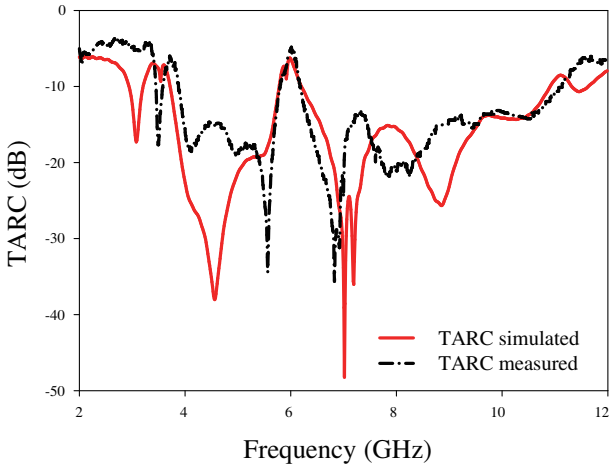

Figure 9. TARC of the proposed dual band notch MIMO antenna.

5.4. Channel Capacity Total

The channel capacity loss is calculated numerically by Equations (5).

$$CCL = -\log_2 det\left(\psi^R\right) \tag{5}$$

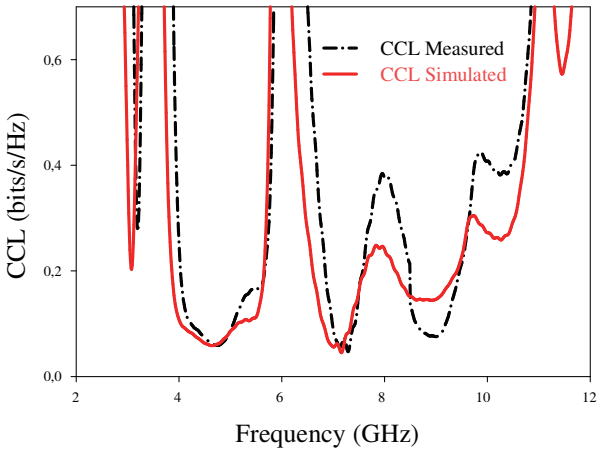

Figure 10. CCL of the proposed UWB MIMO antenna with dual band-notched characteristic.

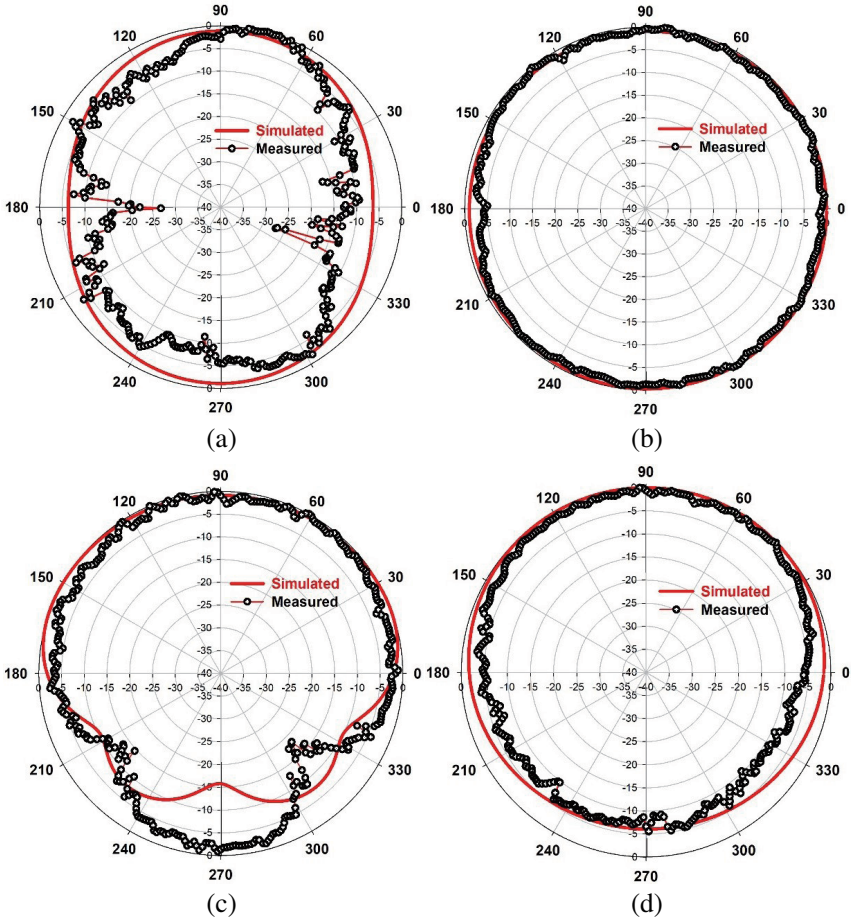

Figure 11. The measured and simulated radiation patterns of the proposed antenna at frequencies: (a) E-plane at 4 GHz, (b) H-plane at 4 GHz, (c) E-plane at 8 GHz, (d) H-plane at 8 GHz.

$\rho_{ii} = 1 - \left| \sum_{n=1}^{M} S_{in}^{*} \times S_{ni} \right|$ and $\rho_{ij} = - \sum_{n=1}^{M} S_{in}^{*} \times S_{nj}$ for $ij = 1, 2 \ldots M$. ρ_{ii} and ρ_{ij} are the correlation coefficients.

In general, the CCL value must be less than 0.4 bits/s/Hz [11] for the entire working range. As shown in Figure 10, the CCL is very good, and its value is less than 0.4 bit/s/Hz in most of the operating band, excluding the notched band at 3.6 GHz and 6 GHz in UWB range.

5.5. Radiation Patterns

The simulated and measured radiation characteristics of the presented antenna at 4 GHz and 8 GHz are illustrated in the Figure 11. From this figure, the radiation patterns of the proposed antenna are almost omnidirectional for the E and H planes to receive the signal from all directions. A good agreement is observed with a little difference between the measured and simulated radiation patterns which is due to the absence of an anechoic chamber.

6. PERFORMANCE COMPARISON

Table 3 summarizes the comparison of the proposed two-port MIMO antenna array with other existing MIMO systems, including size, isolation between the antenna elements, ECC, operating bands, efficiency, and DG. In this Table, it can be noted that the proposed dual band notch UWB MIMO antenna possesses wide impedance bandwidth with smaller dimensions, followed by excellent ECC and DG values.

Table 3. Performance comparison between the proposed structure and other reported works.

Ref. N°	Year	Number of N°	Size (m^{m3}	Isolatio (dB)	EC	Bandwidth (GHz)	Effic. (%)	DG (dB)
[21]	2018	2	30×41	< -20	< 0.1	2.2 GHz to 11 GH	80%	—
[22]	2018	3	58×45	< -15	≤ 0.5	3.1 GHz to 11 GH	80%	—
[23]	2021	2	50×50	< -21	< 0.04	2.36 GHz to12 GH	—	9.99
[24]	2020	2	32×46	< -20	< 0.5	3.1 GHz to 16 GH	—	—
[25]	2018	1	46×46	< -17	0.02	3.1 GHz to 12 GH	75%	—
[26]	2015	2	40×40	< -15	0.5	—	—	—
[27]	2015	1	38.5×38.5	< -15	< 0.02	3.08 GHz to 11.8 GHz	> 75	—
[28]	2014	0	40×40	—		3 GHz to 11 GH	100%	99
[29]	2021	2	40×40	-18	< 0.1	2.3 GHz to 9.96 GH	—	8–9.5
[30]	2014	1	48×48	-15	< 0.005	2.5 GHz to 12 GH	—	—
[31]	2017	1	50×82	-15	< 0.04	2.2 GHz to 13.3 GH	60%	—
P.S	2021	2	40×30	-15	0.02	3.05 GHz to 11.65 GH	58%	9.94

P.S= proposed structure, Effic.=Efficiency

7. CONCLUSION

In this paper, a compact dual band notch UWB MIMO antenna in 5G and Wi-Fi 6E is proposed. The dual band-notched function is achieved by embedding a complementary split ring resonators (CSRR) within the rectangular patch, and a split ring resonator (SRR) is loaded on the ground plane at the back of each patch antenna. Simulated and measured results show that the proposed antenna has broadband impedance bandwidth covering the whole UWB, dual band-notched function with good isolation between two ports, stable radiation patterns, low envelope correlation and CCL<0.4 bits/s/Hz. These results indicate that the developed antenna can be a good candidate for UWB MIMO systems.

ACKNOWLEDGMENT

This work was partially supported by Faculty of Sciences, under Information Systems and Telecommunications Laboratory, Abdelmalek Essaâdi University, Tetuan, Morocco, Supervised by Professor Mohsine Khalladi. The authors would like to thank Professor Naima Amar Touhami of Abdelmalek Essaâdi University, Tetuan, Morocco for providing the measurements facility.

REFERENCES

1. Xu, H. and L. Yang, "Ultra-wideband technology: Yesterday, today, and tomorrow," *2008 IEEE Radio Wirel. Symp.*, 715–718, 2008.
2. Nikookar, H. and R. Prasad, *Introduction to Ultra-wideband for Wireless Communications*, Springer, Netherlands, 2009.
3. Kuhn, V., *Wireless Communications over MIMO Channels: Applications to CDMA and Multiple Antenna Systems*, Engl. John Wiley Sons, 2006.
4. Khan, M. S., A. D. Capobianco, S. Asif, A. Iftikhar, B. Ijaz, and B. D. Braaten, "Compact 4×4 UWB-MIMO antenna with WLAN band rejected operation," *Electron. Lett.*, Vol. 51, No. 14, 5–6, 2015, doi: 10.1049/el.2015.1252.
5. Kayabasi, A., A. Toktas, E. Yigit, and K. Sabanci, "Triangular quad-port multi-polarized UWB MIMO antenna with enhanced isolation using neutralization ring," *AEU — Int. J. Electron. Commun.*, Vol. 85, 47–53, 2018, doi: 10.1016/j.aeue.2017.12.027.
6. Nirmal, P. C., A. Nandgaonkar, S. Nalbalwar, and R. K. Gupta, "Compact wideband MIMO antenna for 4G WI-MAX, WLAN and UWB applications," *AEUE — Int. J. Electron. Commun.*, Vol. 99, 284–292, 2019, doi: 10.1016/j.aeue.2018.12.008.
7. Fletcher, P. N., M. Dean, and A. R. Nix, "Mutual coupling in multi-element array antennas and its influence on MIMO channel capacity," *Electron. Lett.*, Vol. 39, No. 4, 342–344, 2003, doi: 10.1049/el:20030219.
8. Ali, W. A. E. and A. Ibrahim, "A compact double-sided MIMO antenna with an improved isolation for UWB applications," *AEUE — Int. J. Electron. Commun.*, Vol. 82, 7–13, 2017, doi: 10.1016/j.aeue.2017.07.031.
9. Kumar, M., K. Sachin, and B. K. Kanaujia, "Design, modeling and analysis of dual-feed defected ground microstrip patch antenna with wide axial ratio bandwidth," *J. Comput. Electron.*, Vol. 17, No. 03, 1019–1028, 2018, doi: 10.1007/s10825-018-1173-1.
10. Tiwari, R. N., P. Singh, B. K. Kanaujia, and K. Srivastava, "Neutralization technique based two and four port high isolation mimo antennas for UWB communication," *AEUE — Int. J. Electron. Commun.*, Vol. 110, 152828, 2019, doi: 10.1016/j.aeue.2019.152828.
11. Dabas, T., D. Gangwar, B. K. Kanaujia, and A. K. Gautam, "Mutual coupling reduction between elements of UWB MIMO antenna using small size uniplanar EBG exhibiting multiple stop bands," *AEUE — Int. J. Electron. Commun.*, Vol. 93, 32–38, 2018, doi: 10.1016/j.aeue.2018.05.033.
12. Srivastava, K., A. Kumar, B. K. Kanaujia, S. Dwari, and S. Kumar, "A CPW-fed UWB MIMO antenna with integrated GSM band and dual band notches," *Int. J. RF Microw. Comput. Eng.*, Vol. 29, No. 1, 2–6, 2019, doi: 10.1002/mmce.21433.
13. Hassan, M. M., et al., A novel UWB MIMO antenna array with band notch characteristics using parasitic decoupler," *Journal of Electromagnetic Waves and Applications*, Vol. 34, No. 9, 1225–1238, 2020, doi: 10.1080/09205071.2019.1682063.
14. Raheja, D. K., S. Kumar, and B. K. Kanaujia, "Compact quasi-elliptical-self-complementary four-port super-wideband MIMO antenna with dual band elimination characteristics," *AEU — Int. J. Electron. Commun.*, Vol. 114, 153001, 2020, doi: 10.1016/j.aeue.2019.153001.
15. Banerjee, J., A. Karmakar, R. Ghatak, and D. R. Poddar, "Compact CPW-fed UWB MIMO antenna with a novel modified Minkowski fractal defected ground structure (DGS) for high isolation and triple band-notch characteristic," *Journal of Electromagnetic Waves and Applications*, Vol. 31, No. 15, 1550–1565, 2017, doi: 10.1080/09205071.2017.1354727.

16. Mansouri, Z., A. S. Arezomand, S. Heydari, and F. B. Zarrabi, "Dual notch UWB fork monopole antenna with CRLH metamaterial load," *Progress In Electromagnetics Research C*, Vol. 65, 111–119, 2016.
17. Zarrabi, F. B., A. Pirooj, and K. Pedram, "Metamaterial loads used in microstrip antenna for circular polarization: Review," *Int. J. RF Microw. Comput. Eng.*, Vol. 29, No. 10, 1–17, 2019, doi: 10.1002/mmce.21869.
18. Zhang, J., J. Ouyang, K. Z. Zhang, and F. Yang, "A novel dual-band MIMO antenna with lower correlation coefficient," *Int. J. Antennas Propag.*, Vol. 49, No. 10, 2636–2647, 2012, doi: 10.1155/2012/512975.
19. Pierce, J. N. and S. Stein, "Multiple diversity with nonindependent fading," *Proc. IRE*, Vol. 48, No. 1, 89–104, 1960, doi: 10.1109/JRPROC.1960.287384.
20. Schwartz, M., W. R. Bennett, and S. Stein, *Mommunication Systems and Techniques*, 9–10, John Wiley Sons, May 1995.
21. Gorai, A., A. Dasgupta, and R. Ghatak, "A compact quasi-self-complementary dual band notched UWB MIMO antenna with enhanced isolation using Hilbert fractal slot," *AEU — Int. J. Electron. Commun.*, Vol. 94, No. June, 36–41, 2018, doi: 10.1016/j.aeue.2018.06.035.
22. Jaglan, N., S. D. Gupta, B. K. Kanaujia, S. Srivastava, and E. Thakur, "Triple band notched DG-CEBG structure based UWB MIMO/diversity antenna," *Progress In Electromagnetics Research C*, Vol. 80, 21–37, 2018.
23. Zhou, J. Y., Y. F. Wang, J. M. Xu, and C. Z. Du, "A CPW-fed UWB-MIMO antenna with high isolation and dual band-notched characteristic," *Progress In Electromagnetics Research M*, Vol. 102, No. January, 27–37, 2021.
24. Zhang, J., L. Wang, and W. Zhang, "A novel dual band-notched CPW-fed UWB MIMO antenna with mutual coupling reduction characteristics," *Progress In Electromagnetics Research Letters*, Vol. 90, No. December, 21–28, 2020.
25. Debnath, P., A. Karmakar, A. Saha, and S. Huda, "UMB MIMO Slot antenna with minkowski fractal shaped isolators for isolation enhancement," *rogress In Electromagnetics Research M*, Vol. 75, No. September, 69–78, 2018.
26. Zhu, J., B. Feng, B. Peng, S. Li, and L. Deng, "Compact CPW UWB diversity slot antenna with dual band-notched characteristics," *Microw. Opt. Technol. Lett.*, Vol. 55, No. 11, 2562–2568, 2015.
27. Kang, L., H. Li, X. Wang, and X. Shi, "Compact offset microstrip-fed MIMO antenna for band-notched UWB applications," *IEEE Antennas Wirel. Propag. Lett.*, Vol. 14, 1754–1757, 2015, doi: 10.1109/LAWP.2015.2422571.
28. Mao, C. X. and Q. X. Chu, "Compact coradiator UWB-MIMO antenna with dual polarization," *IEEE Trans. Antennas Propag.*, Vol. 62, No. 9, 4474–4480, 2014, doi: 10.1109/TAP.2014.2333066.
29. Mohan Reddy, S. S., B. Sanjay, K. Aruna Kumari, B. T. P. Madhav, and B. Prudhvi Nadh, "MIMO dual sensing antenna with notch characteristics," *J. Phys. Conf. Ser.*, Vol. 1804, No. 1, 012194, 2021, doi: 10.1088/1742-6596/1804/1/012194.
30. Gao, P., S. He, X. Wei, Z. Xu, N. Wang, and Y. Zheng, "Compact printed uwb diversity slot antenna with 5.5-GHz band-notched characteristics," *IEEE Antennas Wirel. Propag. Lett.*, Vol. 13, 376–379, 2014.
31. Toktas, A., "G-shaped band-notched ultra-wideband MIMO antenna system for mobile terminals," *IET Microwaves, Antennas Propag.*, Vol. 11, No. 5, 718–725, 2017, doi: 10.1049/iet-map.2016.0820.